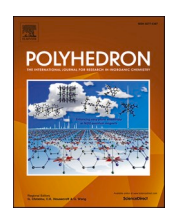


Contents lists available at ScienceDirect

# Polyhedron

journal homepage: www.elsevier.com/locate/poly





# Structurally dynamic crystalline 1D coordination polymers enabled via the Weak-Link Approach

Benjamin D. Coleman, Andrea I. d'Aquino, Zachary Kean, Yihan Wang, Jenny K. Hedlund Orbeck, Charlotte L. Stern, Chad A. Mirkin \*

Department of Chemistry, Northwestern University, Evanston, IL, USA

ARTICLE INFO

Keywords:
Coordination polymers
Weak-Link Approach
Hemilabile ligands
Single-crystal X-ray diffraction
Stimuli-responsive materials

#### ABSTRACT

Supramolecular chemistry has the potential to be used to impart dynamic molecular elements into coordination polymers so that sophisticated, multifunctional materials can be prepared. Indeed, the Weak-Link Approach (WLA) to supramolecular chemistry is a coordination chemistry-based platform that can be used for the design of stimuli-responsive and switchable nanoscale architectures. Herein, we use the WLA to design and synthesize crystalline, WLA-based 1D coordination polymers. Specifically, the reaction of a closed, pyridine-functionalized WLA monomer complex with Cu(BF<sub>4</sub>)<sub>2</sub>·6H<sub>2</sub>O in acetonitrile or *N*,*N*-dimethylformamide yields three isostructural 1D zig-zag chains. One of the polymers was studied via single-crystal X-ray diffraction (SCXRD), nuclear magnetic resonance (NMR) spectroscopy, and mass spectroscopy (MS), and its response to a chemical effector (halide ion, Cl<sup>-</sup>) was investigated. Importantly, our investigation of one of the model chains displays the characteristic structural switchability of the WLA complex from which it is comprised. Upon exposure to Cl<sup>-</sup> anions, it disassembles into its molecular components, including the fully-opened congener of the initial WLA complex. Thus, one can control crystalline chain assembly via the structural state of the WLA monomer complex. Taken together, this work has demonstrated the construction of the first series of crystalline WLA-based extended solids and represents a promising method for the construction of allosteric, stimuli-responsive coordination polymers, including potentially higher-ordered structures like metal organic frameworks.

#### 1. Introduction

Supramolecular interactions are the basis for primary, secondary, and tertiary structures of many biological macromolecules (*e.g.*, proteins). These network interactions permit allosteric regulation, govern stimuli response (*e.g.*, from molecular effectors), and dictate molecular properties [1–4]. Drawing on design principles that occur in nature, researchers have sought to build abiotic architectures with similar features and use them as a basis for next-generation functional materials. To date, many approaches in the field of coordination-driven supramolecular chemistry have been pursued to prepare chemical moieties that vary in their synthetic complexity and applicability [5–22].

In the context of coordination chemistry, the Weak-Link Approach (WLA) has emerged as a powerful method to synthesize supramolecular structures that exhibit allosteric regulation [23–25]. The WLA relies on hemilabile bidentate ligands that feature two moieties with distinct coordination strengths—a coordinatively inert "strong link" (e.g.,

phosphino- or N-heterocyclic carbenes) and a coordinatively labile "weak link" (e.g., ether, amino, thioether). Upon reaction with a d8 transition metal precursor (e.g., RhI, IrI, PdII, PtII), a condensed, squareplanar structure is formed. When the square planar complexes are exposed to halide [26-30] (e.g., Cl and I anions), small molecule effectors [31-35] (e.g., CO, CH<sub>3</sub>CN, amines) or by oxidizing/reducing pendant functionalities [36-43] (e.g., oxidation and reduction of appended ferrocene moieties), the "weak link" is preferentially displaced, allowing the structure to toggle between different structural states (e.g., fully closed, semi-open, and fully open) (Fig. 1). Using the WLA, a variety of supramolecular structures can be accessed, including molecular tweezers [28,29,44,45], macrocycles [26,27,31–35,46,47], and tri-layer structures [48-51]. The modularity, tailorability, and stimuli-responsiveness achieved through the WLA has enabled the design of stimuli-responsive catalysts [48,49], signal amplifiers [46,47], fluorescent probes [44,45], and light-harvesting materials [50,51].

Infinite coordination polymers (ICPs), which consist of multidentate

E-mail address: chadnano@northwestern.edu (C.A. Mirkin).

<sup>\*</sup> Corresponding author.

ligands interconnected via coordination to metal ions to form 1D, 2D, or 3D architectures, represent another promising class of supramolecular materials for the design of stimuli-responsive and abiotic allosteric systems due to their high degree of tunability and ability to be rationally designed [5,52-54]. We hypothesized that by adding pendant functional groups onto the hemilabile ligands that allow for coordination to a secondary metal binding unit (SBU), a new type of WLA monomer complex could be synthesized and polymerized to form stimuliresponsive ICPs. Due to the modularity of the WLA platform, these monomer complexes could be easily adapted to respond to a range of stimuli or display a variety of functions in the resulting ICPs. Previously, we reported the design and synthesis of stimuli-responsive WLA-based ICP particles [55]. In this work, a WLA monomer complex featuring pendant terpyridine moieties was polymerized in the presence of Fe<sup>II</sup> to form amorphous ICP particles. Importantly, this work demonstrates that localized changes to the structure of the embedded WLA monomers regulate the assembly of an extended solid, which can be applied to dictate the chemical and physical properties of an extended ICP material. However, the amorphous nature of the particles precluded a complete crystallographic analysis of the structural transformation induced upon chemical effector binding (e.g., Cl<sup>-</sup> anion), and the extended structure of the material could only be investigated indirectly, thus limiting our ability to identify unambiguous design criterion for the synthesis and characterization of WLA-based ICPs (WLA-ICPs).

Herein, in order to permit further structure-function investigations, we designed, synthesized, and crystallographically characterized three WLA-ICPs. We hypothesized that exchanging the terpyridine moiety for a more coordinately labile functional group (i.e., pyridine) would allow for the controlled assembly of a crystalline solid, while avoiding the formation of kinetically driven, amorphous ICP particles. The reaction of the Pd<sup>II</sup>-phosphino-thioether(P,S)-based WLA monomer complex with a  $Cu^{II}$  precursor ( $Cu(BF_4)_2 \cdot 6H_2O$ ) in a variety of solvents leads to the formation of three independent, but closely related, 1D zig-zag chain compounds, primarily differing in the bound solvent completing the  $\text{Cu}^{\text{II}}$ coordination sphere. We observe that these WLA-ICPs retain the characteristic stimuli-responsiveness of the WLA platform, even after the formation of an extended structure. When representative WLA-ICP crystals were exposed to a Cl<sup>-</sup> anion solution, the extended structure disassembles as Cl- binds to the PdII node of the embedded WLA monomer complex. In this way, one can control crystallization and assembly simply by toggling the structural state of the WLA monomer. Taken together, the three new WLA-ICP chain compounds pursued in this work expand the scope of supramolecular architectures accessible via the WLA platform, and also lay a foundation for a new class of allosteric, stimuli-responsive coordination polymers.

## 2. Material and methods

## 2.1. General methods

Unless otherwise noted, all reactions and procedures were performed

under a dinitrogen atmosphere in a Vacuum Atmospheres Nexus II glovebox or using standard Schlenk techniques. All commercially available chemicals and reagents were purchased and used without further purification, unless otherwise stated. 1,2-Dichloroethane, 0.5 M potassium diphenylphosphide solution in tetrahydrofuran, and tetra(nbutyl)ammonium chloride were purchased from Millipore-Sigma. 4-Mercaptopyridine was purchased from TCI America. Tetrakis(acetonitrile)palladium(II) tetrafluoroborate was purchased from Strem Chemical, and copper(II) tetrafluoroborate hexahydrate was purchased from Alfa Aesar. Tetrahydrofuran (THF), diethyl ether (Et2O), and dichloromethane (DCM) were dried using a commercial solvent purification system purchased from JC Meyer Solvent Systems and deoxygenated under a stream of argon prior to use. Anhydrous acetonitrile (MeCN) and anhydrous N,N-dimethylformamide (DMF) were purchased from Millipore-Sigma. Anhydrous methanol (MeOH) was purchased from Thermo Scientific. (2-Chloroethyl)diphenylphosphine was synthesized according to literature methods [56]. Filtrations were performed by gravity through a Whatman medium to fine mesh filter paper using a Büchner funnel. Flash chromatography was performed using a silica gel column (60 Å pore size, 230–400 mesh ASTM, 0.040–0.063 mm; Fluka). Vapor diffusion for crystal growth was conducted by sealing a culture tube containing 300 µL of the growth solution in a 20-mL scintillation vial containing approx. 4 mL of Et<sub>2</sub>O. The sealed vial was allowed to stand in the glovebox at 25 °C during crystal growth. Sample sonication for NMR experiments were performed in a 25 °C water bath in a Branson Ultrasonic M2800 sonicator. Deuterated solvents (CD2Cl2, CD3CN) were purchased from Cambridge Isotope Laboratories. 1H, 31P{1H}, and DOSY NMR spectra were collected on a Bruker Advance 400 MHz NMR spectrometer at 298 K under ambient conditions, and chemical shifts (δ) are given in parts per million (ppm). <sup>1</sup>H NMR spectra were referenced to residual solvent proton resonances ( $CD_2Cl_2 = \delta$  5.32;  $CD_3CN = \delta$  1.94), and <sup>31</sup>P{<sup>1</sup>H} NMR spectra were indirectly referenced via <sup>31</sup>P gyromagnetic ratio. Electron-spray ionization mass spectrometry (ESI-MS) data were collected using a Bruker amaZon SL equipped with Hystar Version 3.2 data acquisition software. ESI-MS data were subsequently processed and analyzed using Compass Version 4.4. The mass spectrometer was configured with an Agilent 1100 Series HPLC module with an ESI source and 3D ion trap mass analyzer. The samples were analyzed with a 3-µL injection volume, and the mobile phase composition was 100 % MeCN. Data were collected in positive ion mode. High resolution mass spectra were obtained on an Agilent 6230 Time of Flight Mass Spectrometer attached to an Agilent 1200 series HPLC stack. Data were acquired on Agilent Mass Hunter Acquisition software and analyzed on Agilent Mass Hunter Qualitative Analysis software. Powder X-ray diffraction (PXRD) data were collected at room temperature on a STOE-STADI-P powder diffractometer equipped with an asymmetric curved Germanium monochromator (CuK $\alpha$ 1 radiation,  $\lambda = 1.54056$  Å) and one-dimensional silicon strip detector (MYTHEN 21K and DECTRIS). The line focused Cu X-ray tube was operated at 40 kV and 40 mA. Powder was packed in a 3mm metallic disk purchased from STOE and sandwiched between two layers of polyimide tape. Diffraction data were collected from 5 to 55°  $2\theta$ 

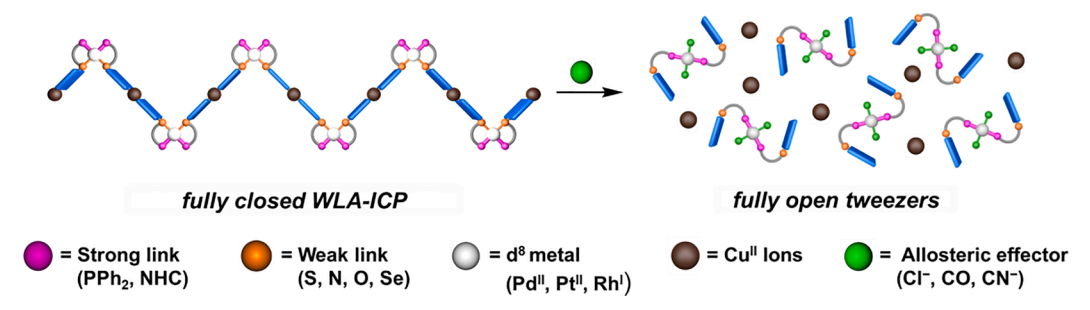


**Fig. 1.** The Weak-Link Approach to supramolecular chemistry utilizes hemilabile ligands coordinated to d<sup>8</sup> transition metal ions to generate a toggleable structural node. Upon exposure to chemical and physical stimuli, small molecule or anionic effectors preferentially displace the more labile "weak-link", resulting in a more open, flexible structure.

over 10 min. The instrument was calibrated against a NIST silicon standard (640d) prior to measurement. CHN analysis was conducted in triplicate by Midwest Microlab, LLC (Indianapolis, IN).

#### 2.2. Syntheses

Hemilabile P,S-pyridine(pyr) Ligand (1). Diphenyl((4-pyridyl) thioethyl)phosphine was synthesized via modification of literature procedures for previously reported analogous compounds [25,50,57-59]. In a glovebox under an inert atmosphere, (2-chloroethyl)diphenylphosphine (294.5 mg, 1.184 mmol), 4-mercaptopyridine (117.3 mg, 1.055 mmol), and cesium carbonate (674.3 mg, 2.070 mmol) were combined in 5 mL of MeCN in a 10-mL scintillation vial equipped with a magnetic stir bar. The vial was sealed with a cap and electrical tape, removed from the glovebox, and stirred at 75 °C overnight. Purification was then conducted under aerobic conditions. The reaction mixture was cooled to room temperature, filtered to remove cesium chloride and excess cesium carbonate, and the solvent was removed in vacuo to afford a yellow oil. The oil was purified by column chromatography on a silica gel using a 0-100 % DCM/MeOH gradient, and the solvent was removed in vacuo to afford the desired hemilabile ligand 1 as an off-white solid (268.6 mg, 79 % yield). <sup>1</sup>H NMR (400 MHz, CD<sub>2</sub>Cl<sub>2</sub>)  $\delta$  8.33 (d, J = 5.4 Hz, 2H),  $\delta$  7.55–7.35 (m, 10*H*),  $\delta$  7.06–6.95 (m, 2H),  $\delta$  3.15–3.02 (m, 2H),  $\delta$  2.50–2.40 (m, 2H).  $^{31}P\{^{1}H\}$  NMR (162 MHz, CD<sub>2</sub>Cl<sub>2</sub>)  $\delta$  –17.32. MS (ESI+) m/z Calculated for  $[1+H]^+$   $C_{19}H_{19}N_1P_1S_1$ : 324.0976. Found: 324.10.

WLA Monomer Complex [Pd(P,S-pyr)<sub>2</sub>] [(BF<sub>4</sub>)<sub>2</sub>] (2). Hemilabile ligand 1 (333.9 mg, 1.032 mmol) was dissolved in 2 mL of DCM and was added dropwise to a stirring slurry of tetrakis(acetonitrile)palladium(II) tetrafluoroborate (230.4 mg, 0.5186 mmol) in 2 mL of MeOH in a 10-mL scintillation vial. During the addition, a yellow precipitate was observed within minutes. The reaction was stirred overnight, and then the solution was removed from the glovebox and filtered, yielding a homogenous orange solution. Et<sub>2</sub>O was added to the solution to precipitate a pale-yellow solid. The solid was collected via filtration, washed three times with excess Et<sub>2</sub>O, and dried *in vacuo* resulting in the desired metal complex as a pale-yellow solid (375.5 mg, 77 % yield).  $^1$ H NMR (400 MHz, CD<sub>3</sub>CN)  $\delta$  8.70 (s, 5H),  $\delta$  7.68–7.38 (m, br, 27H),  $\delta$  3.32 (s, br, 8H).  $^{31}$ P{ $^1$ H} NMR (162 MHz, CD<sub>3</sub>CN)  $\delta$  63.64. HR-MS (ESI+) m/z Calculated for [2–BF $^-$ ] $^+$  C<sub>38</sub>H<sub>36</sub>BF<sub>4</sub>N<sub>2</sub>P<sub>2</sub>PdS<sub>2</sub>: 839.0859. Found: 839.0893.

 $[Cu(Pd(P,S-pyr)_2)(MeCN)_4][(BF_4)_4]$  (3<sup>MeCN</sup>). WLA monomer complex 2 (201.0 mg, 0.217 mmol) and Cu(BF<sub>4</sub>)<sub>2</sub>·6H<sub>2</sub>O (74.0 mg, 0.214 mmol) were combined in 4 mL of MeCN in a 10-mL scintillation vial, and a dark- green homogenous solution formed. This solution was left to stand at 25 °C for 3 days in the glovebox, during which blue-green, block crystals, suitable for X-ray crystallographic characterization, grew upon the walls of the vial. After the 3 days, the mother liquor was decanted via pipette, and the crystals were washed with MeCN (3 × 1 mL) before being stored under a minimal amount of MeCN (approx. 250 μL) (99.5 mg, 26 %). Anal. Calcd. for  $C_{46}H_{48}B_4CuF_{16}N_6P_2PdS_2$ : C 41.6, H 3.64, N 6.33 %. Found: C  $36.7\pm0.187,\, H~3.44\pm0.085,\, N~2.96\pm0.116$  %. The lower CHN percentages observed for 3<sup>MeCN</sup> versus the calculated are attributed to partial loss of bound MeCN solvent molecules during high vacuum drying. The crystals were dissolved in 1 g CD<sub>3</sub>CN for NMR analysis via sonication at 25  $^{\circ}\text{C}.$  Due to the coordination of paramagnetic  $d^{9}$   $\text{Cu}^{\text{II}}$ ions, <sup>1</sup>H NMR resonances corresponding to the protons in the pyridine moiety have shifted outside the spectral window and could not be observed upon expanding to 100 ppm.  $^{1}$ H NMR (400 MHz, CD $_{3}$ CN)  $\delta$ 7.66–7.36 (m, br, 20H),  $\delta$  3.23 (s, br, 8H).  $^{31}P\{^{1}H\}$  NMR (162 MHz, CD<sub>3</sub>CN)  $\delta$  61.76.

[Cu(Pd(P,S-pyr)<sub>2</sub>)(H<sub>2</sub>O)(MeCN)<sub>3</sub>] [(BF<sub>4</sub>)<sub>4</sub>]  $\bullet$ H<sub>2</sub>O $\bullet$ MeCN (3<sup>H<sub>2</sub>O</sup>). WLA monomer complex **2** (46.9 mg, 0.0506 mmol) and Cu(BF<sub>4</sub>)<sub>2</sub>·6H<sub>2</sub>O (39.0 mg, 0.113 mmol) were each separately dissolved in 1 mL of MeCN, before combining them to form a 2-mL dark-green solution that was left

to stand in the glovebox at 25  $^{\circ}$ C overnight. Then, Et<sub>2</sub>O was allowed to slowly diffuse into the solution. After 24 h, yellow, plate-like crystals suitable for single crystal X-ray analysis were obtained. The resulting crystals were stored in their growth solution.

[Cu(Pd(P,S-pyr)<sub>2</sub>)(DMF)<sub>4</sub>] [(BF<sub>4</sub>)<sub>4</sub>] ( $3^{DMF}$ ). Analogous to the preparation of  $3^{MeCN}$ , WLA complex 2 (119.0 mg, 0.129 mmol) and Cu (BF<sub>4</sub>)<sub>2</sub>·6H<sub>2</sub>O (46.9 mg, 0.136 mmol) were combined in 3 mL of DMF in a 10-mL scintillation vial, and a yellow, homogenous solution formed. After allowing this solution to stand at 25 °C for 6 days in the glovebox in which it was prepared, Et<sub>2</sub>O was allowed to slowly diffuse into solution. After 2 weeks, green, block crystals suitable for single crystal X-ray analysis were obtained. The resulting crystals were stored in their growth solution.

*In Situ* Reaction of Cl<sup>-</sup> anion with 3<sup>MeCN</sup>. To a slurry consisting of crystals of 3<sup>MeCN</sup> (39.0 mg, 0.0294 mmol) in 1 g of CD<sub>3</sub>CN, a solution of tetra(n-butyl)ammonium chloride (49.2 mg, 0.177 mmol) in 1 g of CD<sub>3</sub>CN was added at 25 °C. Immediately upon addition, the supernatant turned from colorless to yellow, and the blue-green crystals of 3<sup>MeCN</sup> expanded and changed into a white powder. The reaction mixture was allowed to stand overnight at 25 °C in the glovebox in which it was prepared, at which point all of the crystals were consumed and transformed into an off-white solid in a yellow solution. An aliquot of the crude reaction solution was transferred to an air-free NMR tube and analyzed by <sup>1</sup>H and <sup>31</sup>P{<sup>1</sup>H} NMR spectroscopy. Accurate integration of the <sup>1</sup>H NMR resonances is not possible due to the large excess of tetra(nbutyl)ammonium cations in the crude reaction solution. <sup>1</sup>H NMR (400 MHz, CD<sub>3</sub>CN)  $\delta$  7.81–7.36 (m),  $\delta$  3.31–3.25 (m),  $\delta$  3.18–3.05 (m),  $\delta$ 2.95–2.88 (m),  $\delta$  1.63 (tt, J = 8.2, 6.1 Hz),  $\delta$  1.38 (h, J = 7.4 Hz),  $\delta$  1.00 (t, J = 7.3 Hz). <sup>31</sup>P{<sup>1</sup>H} NMR (162 MHz, CD<sub>3</sub>CN)  $\delta$  28.28,  $\delta$  26.94,  $\delta$ 16.01. Under aerobic conditions, the crude white solid was collected via filtration, washed with excess Et<sub>2</sub>O, and dried in vacuo. <sup>1</sup>H NMR (400 MHz,  $CD_2Cl_2$ )  $\delta$  7.74–7.57 (m, br, 28H),  $\delta$  2.83 (s, br, 8H).  $^{31}P\{^{1}H\}$ NMR (162 MHz, CD<sub>2</sub>Cl<sub>2</sub>)  $\delta$  23.08,  $\delta$  16.21.

## 2.3. X-ray structure determination

Single crystals of  $3^{MeCN}$  and  $3^{DMF}$  were mounted on a MiTeGen loop, respectively, with paratone oil on a XtaLAB Synergy diffractometer equipped with a micro-focus sealed X-ray tube PhotonJet (Mo) X-ray source and a Hybrid Pixel Array Detector (HyPix) detector. The temperature of the crystals was controlled with an Oxford Cryosystems low-temperature device. Data reduction was performed with the CrysAlisPro Software using a numerical ( $3^{MeCN}$ ) or spherical ( $3^{DMF}$ ) adsorption correction. The structures were solved with the ShelXT [60] structure solution program using the Intrinsic Phasing solution method and Olex2 [61] as the graphical interface. The model was refined with ShelXL [62] using least squares minimization.

Single crystals of  $3^{H_2O}$  were mounted on a glass fiber with paratone oil on a Kappa Apex 2 diffractometer. The temperature of the crystals was controlled with an Oxford Cryosystems low-temperature device. Data reduction was performed with the Bruker SAINT software package using a numerical adsorption correction. The structure was solved with the ShelXT [60] structure solution program using Direct Methods and Olex2 [61] as the graphical interface. The model was refined with ShelXL [62] using least squares minimization.

## 2.4. Diffusion ordered spectroscopy investigation of ${\bf 2}$ and ${\bf 3}^{\text{MeCN}}$

A 9.4 mg sample of **2** and  $3^{MeCN}$  were dissolved in 1 g CD<sub>3</sub>CN, respectively, for data collection. The samples of  $3^{MeCN}$  were sonicated until a homogenous solution was obtained. Diffusion coefficients were obtained from a peak-by-peak fit to a three-component exponential of the Stejskal-Tanner equation for each proton resonance using the Mestrelab Research MestReNova v14.2.3. software package and reported as a range for each compound.

## 2.5. NMR degradation investigation of $3^{MeCN}$

Inside a glovebox under an inert atmosphere, single crystals of  $3^{MeCN}$  (4.5 mg, 0.0034 mmol) were sealed in an air-free NMR tube under 1 g CD<sub>3</sub>CN.  $^{1}$ H and  $^{31}$ P{ $^{1}$ H} NMR spectra were obtained approximately every 24 h for 14 days. Prior to data collection, the NMR solution was mixed by inverting the NMR tube 3 times before allowing the crystals to settle to the bottom. After 4 days, the  $3^{MeCN}$  crystals were fully dissolved.

### 3. Results and discussion

## 3.1. Synthesis and characterization of $3^{MeCN}$ , $3^{DMF}$ , and $3^{H_2O}$

A primary goal of this work was to use the WLA to synthesize crystalline forms of ICPs, so their extended structures could be studied crystallographically. We view this as a first step toward understanding how to move the WLA system towards higher dimensional extended solids, including metal organic frameworks (MOFs). We hypothesized that, by utilizing a more coordinatively labile pyridine moiety ( $K_a \sim 10^4$  to  $Cu^{II}$ ) [63,64], as opposed to the previously employed terpyridine moiety ( $K_a \sim 10^8$  to  $Fe^{II}$ ) [65], the formation of kinetically trapped amorphous ICP particles would be less likely and an extended, crystalline material could be obtained. To test this hypothesis, a  $Pd^{II}$ -based WLA coordination complex featuring a hemilabile P,S ligand appended with coordinating pyridine functionalities (P,S-pyr, 1) was prepared, and characterized by NMR (Scheme 1).

Given the high affinity of Cu<sup>II</sup> for pyridine and the variety of crystalline ICP structure-types accessible via Cu<sup>II</sup>-pyridine coordination, we studied the interaction of Cu<sup>II</sup> metal ions in the presence of monomer complex 2 (Fig. 2a) [66-73]. Single-crystal X-ray diffraction (SCXRD) was used to confirm that the WLA-based ICP 3<sup>MeCN</sup> crystallizes in the monoclinic centrosymmetric space group P2/n. Each WLA subunit is coordinated to one crystallographically unique Cu<sup>II</sup> metal center to form an alternating 1D linear chain with a zig-zag-like crystal packing (Fig. 2b, Table 1, Fig. S1). The Pd<sup>II</sup> node in each WLA subunit adopts a strained square planer geometry, and the bond angles are described in Table 2 (Fig. 2c). The Pd1-S1-N1 bond angle of 105.83(5)° gives the compound a distinctive zig-zag structure. The Cu<sup>II</sup> SBU assumes an octahedral geometry, where two pyridine moieties from independent WLA subunits adopt a trans configuration (Fig. 2d), and the remaining Cu<sup>II</sup> coordination sites are filled with bound MeCN solvent. As is common to many Cu<sup>II</sup> octahedral compounds, the axially bound MeCN molecules are significantly tetragonally distorted (Table 3). Finally, the cationic ICPs are charge balanced by disordered [BF4] anions that reside in the limited interchain region. When DMF is substituted for

MeCN as the solvent and  $\rm Et_2O$  is allowed to subsequently diffuse into the reaction mixture, green, block crystals of WLA-ICP  $\rm 3^{DMF}$  are accessed (Fig. 3a–c, Tables 1–3). After solvent substitution and diffusion,  $\rm 3^{DMF}$  crystallizes in the  $\rm P2/n$  space group, confirming that this system prefers to form 1D zig-zag chains.

By simply changing the equivalents of Cu<sup>II</sup> in the reaction mixture, a closely related, yet independent, structure was obtained.  $3^{H_2O}$  crystallizes in the monoclinic centrosymmetric space group P2<sub>1</sub>/n and, consistent with  $3^{MeCN}$  and  $3^{DMF}$ , forms 1D zig-zag chains (Fig. 3d, Table 1). Again, the WLA subunit displays a strained square-planar geometry around the PdII node (Fig. 3e, Table 2). However, unlike the other structures,  $3^{H_2O}$  possesses two crystallographically independent octahedral Cu<sup>II</sup> SBUs in its asymmetric unit (Fig. 3f). The first Cu1 coordination sphere features two trans pyridine moieties, two trans water molecules, and two axial, trans acetonitrile molecules. As with  $\mathbf{3}^{MeCN}$  and  $\mathbf{3}^{DMF}$ ,  $\mathbf{3}^{H_2O}$  features a tetragonal distortion of the MeCN ligands (Table 3). The second Cu2 coordination sphere features two trans pyridine moieties and MeCN completes its coordination sphere, and again, features a tetragonal distortion of the bound MeCN molecules. Together, these structures represent the first three crystallographically characterized WLA-based ICPs and show that by carefully controlling the coordination strength of the pendant functionalities to transition-metalbased SBUs, closed WLA complexes can be assembled into crystalline extended structures.

## 3.2. Solvent effects on the structure of $3^{MeCN}$

Next, the WLA subunit's ability to modulate the structure of an extended solid upon chemical effector binding was studied; specifically, the stimuli responsiveness of  $3^{MeCN}$  in solution was explored. To ensure that any structural transformations arose primarily from chemical changes to the WLA metal node and not from solvent effects, the solution structure and solvent stability of the synthesized crystals in MeCN was investigated. Due to challenges growing high quality crystals in bulk quantities for  $3^{DMF}$  and  $3^{H_2O}$ , we focused the remainder of our analysis on  $3^{MeCN}$  given the ease in which robust crystals of this compound could be grown.

To understand the size and length of the  $3^{MeCN}$  structure in solution, DOSY measurements were performed. The DOSY spectrum of monomer complex **2** revealed a diffusion coefficient range of  $D=0.922-1.01\times10^{-5}~{\rm cm}^2/{\rm s}$  by fitting to individual proton resonances (Fig. 4a, Figs. S3–S8). Compound  $3^{MeCN}$  was found to have a smaller diffusion coefficient  $D=6.75-7.17\times10^{-6}~{\rm cm}^2/{\rm s}$ , consistent with  $3^{MeCN}$  having a larger oligomeric structure in comparison to **2** (Fig. 4b, Fig. S9–S12). In agreement with the DOSY measurements, the ESI-MS

Scheme 1. The synthesis of hemilabile ligand (P,S)-pyr (1) and molecular complex [Pd(P,S-pyr)<sub>2</sub>][(BF<sub>4</sub>)<sub>2</sub>] (2).

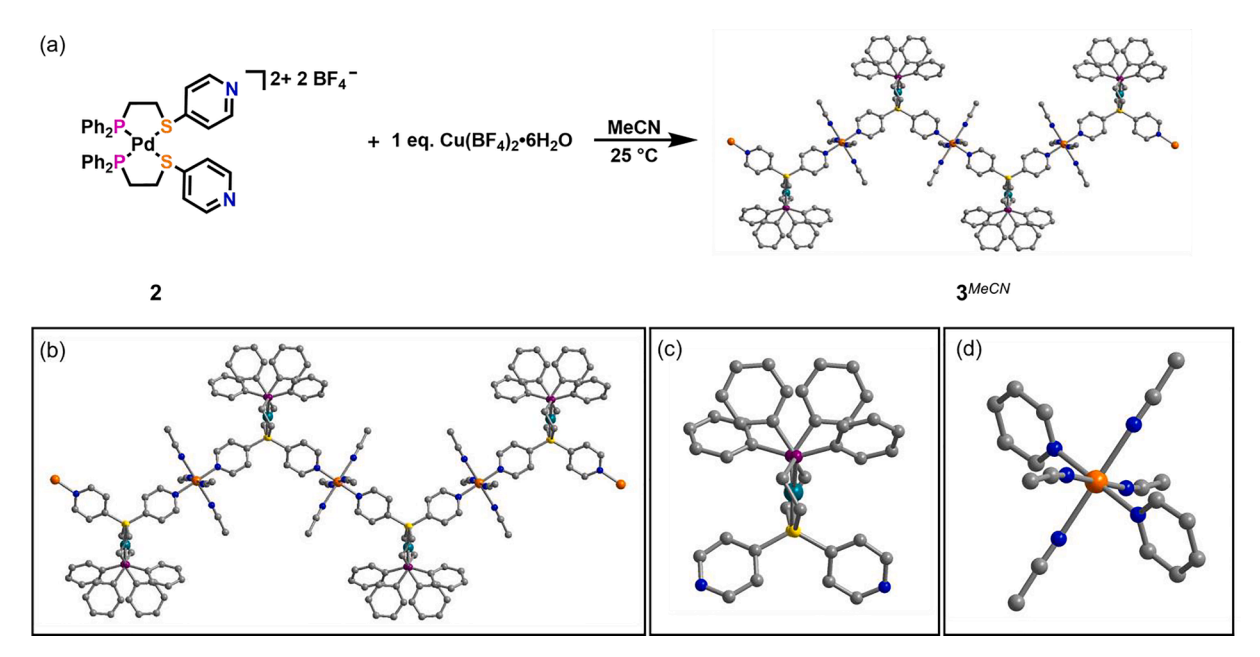


**Fig. 2.** (a) Reaction scheme for the synthesis of coordination polymer  $3^{MeCN}$ . X-ray crystal structure of  $3^{MeCN}$  highlighting (b) the full linear chain, (c) the closed WLA coordination node, and (d) the Cu<sup>II</sup> coordination sphere. Orange, green, purple, yellow, blue, and grey spheres represent Cu, Pd, P, S, N, and C atoms, respectively. Charge balancing counter ions and H atoms have been omitted for clarity. (For interpretation of the references to colour in this figure legend, the reader is referred to the web version of this article.)

Table 1 Crystallographic data for  $3^{MeCN}$ ,  $3^{DMF}$ , and  $3^{H_2O}$ .

	$3^{ m MeCN}$	$3^{\mathrm{DMF}}$	$3^{H_2O}$
Empirical Formula	C <sub>46</sub> H <sub>48</sub> B <sub>4</sub> CuF <sub>16</sub> N <sub>6</sub> P <sub>2</sub> PdS <sub>2</sub>	$C_{50}H_{64}B_4CuF_{16}N_6O_4P_2PdS_2$	C <sub>46</sub> H <sub>50</sub> B <sub>4</sub> CuF <sub>16</sub> N <sub>6</sub> O <sub>2</sub> P <sub>2</sub> PdS <sub>2</sub>
Formula Weight	1328.14	1456.31	1362.16
Temperature/K	100.0(2)	200(2)	100.09
Crystal System	monoclinic	monoclinic	monoclinic
Space Group	P2/n	P2/n	P2 <sub>1</sub> /n
a/Å	13.3938(3)	13.6114(2)	13.3903(4)
b/Å	15.4971(3)	16.1404(2)	30.8825(9)
c/Å	14.5948(4)	14.6275(3)	14.3575(4)
α/°	90	90	90
β/°	106.664(3)	103.577(2)	106.5840(15)
γ/°	90	90	90
Volume/Å <sup>3</sup>	2902.15(12)	3123.76(9)	5690.2(3)
Z	2	2	4
$ ho_{calc}/g~cm^{-3}$	1.520	1.548	1.590
$\mu/\text{mm}^{-1}$	0.893	0.841	0.915
F(000)	1334.0	1478.0	2740.0
Crystal size/mm <sup>3</sup>	$0.119 \times 0.096 \times 0.081$	$0.229 \times 0.14 \times 0.05$	$0.181 \times 0.067 \times 0.024$
Radiation	Mo K $\alpha$ ( $\lambda = 0.71073$ )	Mo K $\alpha$ ( $\lambda = 0.71073$ )	Mo Kα ( $\lambda = 0.71073$ )
20 Range for Data Collection/°	3.924 to 67.768	3.98 to 67.746	3.24 to 56.822
Index Ranges	$-17 \le h \le 20$	$-19 \le h \le 20$	$-17 \le h \le 17$
	$-23 \le k \le 23$	$-22 \le k \le 24$	$-35 \leq k \leq 41$
	$-21 \le l \le 22$	$-22 \le l \le 22$	$-19 \le l \le 19$
Reflections Collected	49,265	110,820	76,641
Independent Reflections	10,356 [ $R_{int} = 0.0522$ , $R_{sigma} = 0.0403$ ]	$11,665 [R_{int} = 0.0395,$	$14,219 [R_{int} = 0.0565,$
	, and a signal	$R_{\text{sigma}} = 0.0268$	$R_{\text{sigma}} = 0.1230]$
Data/Restraints/Parameters	10,356/98/438	11,665/519/544	14,219/141/741
Goodness-of-fit on F <sup>2</sup>	1.084	1.040	1.050
Final R indexes [I>=2σ (I)]	$R_1 = 0.0661, wR_2 = 0.1827$	$R_1 = 0.0498$ , $wR_2 = 0.1349$	$R_1 = 0.0720, wR_2 = 0.1879$
Final R indexes [all data]	$R_1 = 0.0785, wR_2 = 0.1901$	$R_1 = 0.0712, wR_2 = 0.1504$	$R_1 = 0.1164, wR_2 = 0.2033$
Largest diff. peak/hole / $e \ \mathring{A}^{-3}$	1.86/-1.27	1.71/-0.79	1.33/–1.15

spectrum of  $3^{MeCN}$  showed distinct peaks up to 2168.40 m/z (Fig. S25). These results indicate  $3^{MeCN}$  is a distinct species from 2 and, while an ICP in the solid state, is oligomeric (*i.e.*, dimers, trimers) when dissolved into solution via sonication for NMR analysis.

In order to distinguish the solvent contributions from chemical effector (Cl $^-$  anion) exposure, the long-term stability (i.e., over several days) of single crystals of  ${\bf 3}^{MeCN}$  in MeCN was investigated. The first  $^{31}$ P

 $\{^1H\}$  NMR spectrum obtained during this study was consistent with the initial spectrum observed during the characterization of the solution structure of  $3^{MeCN}$  (Fig. 4c, Figs. S13, S14). After 4 days, the crystals of  $3^{MeCN}$  fully dissolved into the deuterated MeCN solution and the first signs of degradation were observable in the  ${}^{31}P\{^1H\}$  spectrum on the fifth day. This degradation continues over the course of the next three days (8 days in total) as  $3^{MeCN}$  fully degrades into a combination of

**Table 2** Selected bond angles (°) for  $3^{MeCN}$ ,  $3^{DMF}$ , and  $3^{H_2O}$ 

selected bond angles ( ) for 3 , 3 , and 3 .					
	3 <sup>MeCN</sup>	$3^{\mathrm{DMF}}$	3 <sup>H2O</sup>		
P1-Pd1-S1	86.02(3)	85.93(2)	85.39(5)		
S1-Pd1-S1	92.50(5)	91.68(3)			
P1-Pd1-P1	95.48(5)	96.49(3)			
Pd1-S1-N1	105.83(5)	110.44(4)			
P2-Pd1-S2			85.51(5)		
P1-Pd1-P2			95.38(6)		
S1-Pd1-S2			93.82(5)		
Pd1-S1-N1			110.89(7)		
Pd1-S2-N4			102.86(7)		

**Table 3** Selected bond lengths (Å) for  $3^{MeCN}$ ,  $3^{DMF}$ , and  $3^{H_2O}$ .

	•		
	$3^{\mathrm{MeCN}}$	$3^{\mathrm{DMF}}$	$3^{H_2O}$
Cu1-N1	2.003(3)	2.049(2)	1.990(4)
Cu1-N2	2.367(5)		2.440(7)
Cu1-N3	2.025(4)		
Cu1-O1		2.246(4)	1.997(5)
Cu1-O2		1.974(3)	
Cu2-N4			1.997(4)
Cu2-N5			2.021(7)
Cu2-N6			2.399(7)

products. The DOSY and degradation experiments illustrate two important behaviors of  $3^{MeCN}$  that are relevant to subsequent studies: (1)  $3^{MeCN}$  is an oligomer in solution, and (2) single crystals of  $3^{MeCN}$  do not degrade sufficiently or quickly enough that changes in structure during the reaction with  $Cl^-$  anions can be attributed to solvent effects alone.

### 3.3. Structural dynamics in the presence of Cl

A key feature of the WLA is its ability to be used to induce structural transformations in supramolecular materials upon small molecule or halide effector binding. After establishing the stability of  $3^{MeCN}$  crystals in MeCN, we investigated their response to Cl<sup>-</sup> anion exposure. Upon exposure to the  $\mathrm{Cl}^-$  solution, the mother liquor turned from colorless to yellow, and within one minute, the blue-green crystals began to expand and turn into an amorphous white powder, consistent with the lack of signal in the PXRD diffractogram (Fig. 5a, Fig. S2, Video S1); the transformation was complete after 24 h, as determined by the disappearance of the <sup>31</sup>P{<sup>1</sup>H} NMR resonance of the chain compound in solution. The two products (i.e., yellow supernatant, and white powder) were both analyzed by <sup>1</sup>H and <sup>31</sup>P{<sup>1</sup>H} NMR spectroscopy. In the <sup>31</sup>P {<sup>1</sup>H} NMR spectrum of the crude white powder, the signal at approx. 16 ppm is assigned to the fully open complex **2**<sup>2Cl</sup> (Fig. 5b, Fig. 6), which is consistent with data from isoelectronic model compounds [28,33,74]. The resonance at approx. 16 ppm in the <sup>31</sup>P{<sup>1</sup>H} NMR spectrum of the yellow solution is assigned to the fully open congener of complex  $2^{2Cl}$ , and the resonance at approx. 28 ppm is assigned to a related fully open species in which the complex is coordinated by two MeCN solvent molecules (2<sup>2MeCN</sup>, Fig. 5c, Fig. 6), consistent with model complexes from the literature [28,33,74]. Given that the crude reaction mixtures were analyzed in situ to capture all reaction products, these analyses resulted in signals in the NMR spectra that we were unable to fully assign (Fig. 5b, c, S15-S18). Attempts to grow crystals suitable for structure determination from the reaction mixtures were unsuccessful. Nevertheless, the in situ NMR experiments suggest that upon exposure to Clanion, the embedded WLA subunits of 3<sup>MeCN</sup> begin to open as the halide binds to the  $Pd^{\mathrm{II}}$  metal centers and along the chain backbone. This structure of the sample transforms from crystalline to amorphous, leading to the complete consumption of the chain crystals, and yielding a mixture of fully open WLA complexes and other products. These experiments demonstrate that even in a rigid, crystalline system, the WLA

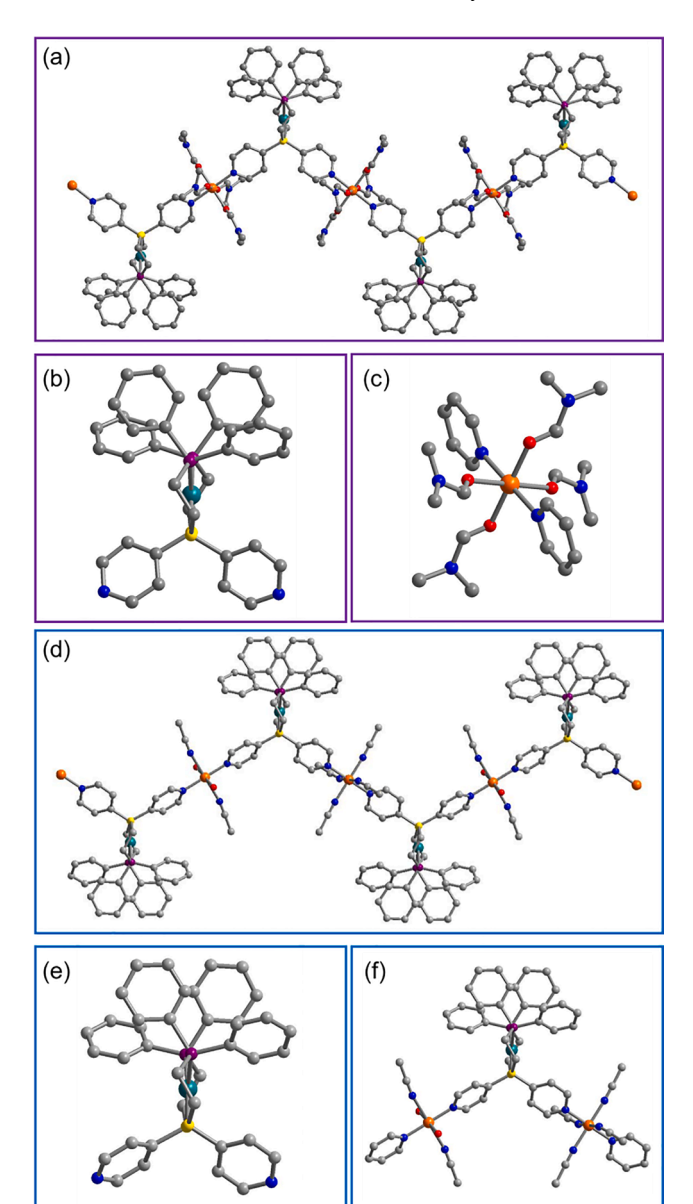


**Fig. 3.** (a) X-ray crystal structure of  $3^{DMF}$  highlighting the full linear chain, (b) the closed WLA coordination node, and (c) the  $Cu^{II}$  coordination sphere. (d) X-ray crystal structure of  $3^{H_2O}$  highlighting the full linear chain, (e) the closed WLA coordination node, and (f) the asymmetric unit including the complete coordination spheres of  $Pd^{II}$  and the two crystallographically unique  $Cu^{II}$  sites. Orange, green, purple, yellow, red, blue, and grey spheres represent Cu, Pd, P, S, O, N, and C atoms, respectively. Charge balancing counter ions, unbound solvent molecules, and H atoms have been omitted for clarity. Modelled rotational disorder of the bound DMF molecules has been omitted for clarity. (For interpretation of the references to colour in this figure legend, the reader is referred to the web version of this article.)

can be used to impart stimuli-responsiveness into supramolecular structures and control the assembly and switching of metalloligands between an extended structure and molecular monomers.

From this data, coupled with SCXRD structures, we postulate a design criterion for next-generation WLA-ICPs: increasing the coordination strength between the WLA monomer and the transition metal SBU will yield materials that maintain crystallinity through the structural transformation. Moving forward, one could envision a WLA-based ICP that could be switched between two crystalline phases to permit the development of design rules for next generation stimuli-responsive materials.

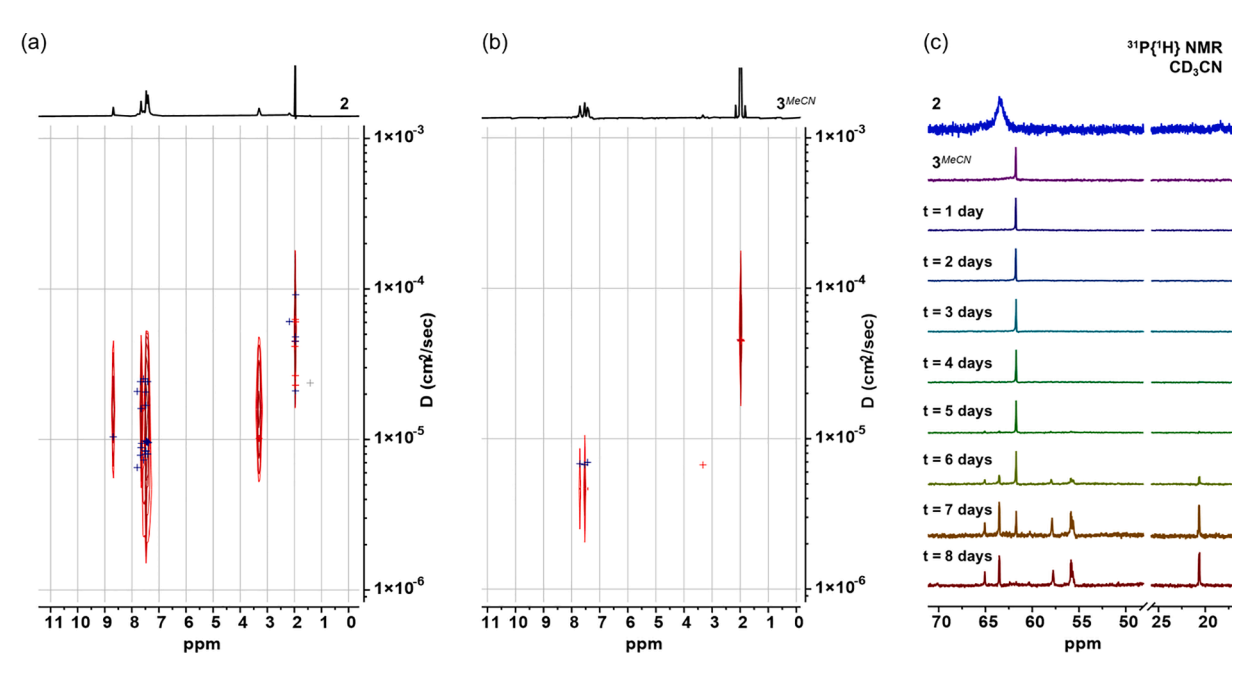


Fig. 4. Psuedo-2D DOSY NMR of (a) 2 and (b)  $3^{MeCN}$ . (c)  ${}^{31}P{}^{1}H{}$  NMR spectra of a mixture containing crystals of  $3^{MeCN}$  soaked in 1 g of solvent in an air-tight NMR tube over the course of 8 days, showing the degradation of the coordination polymer in solution. All spectra were collected in CD<sub>3</sub>CN.

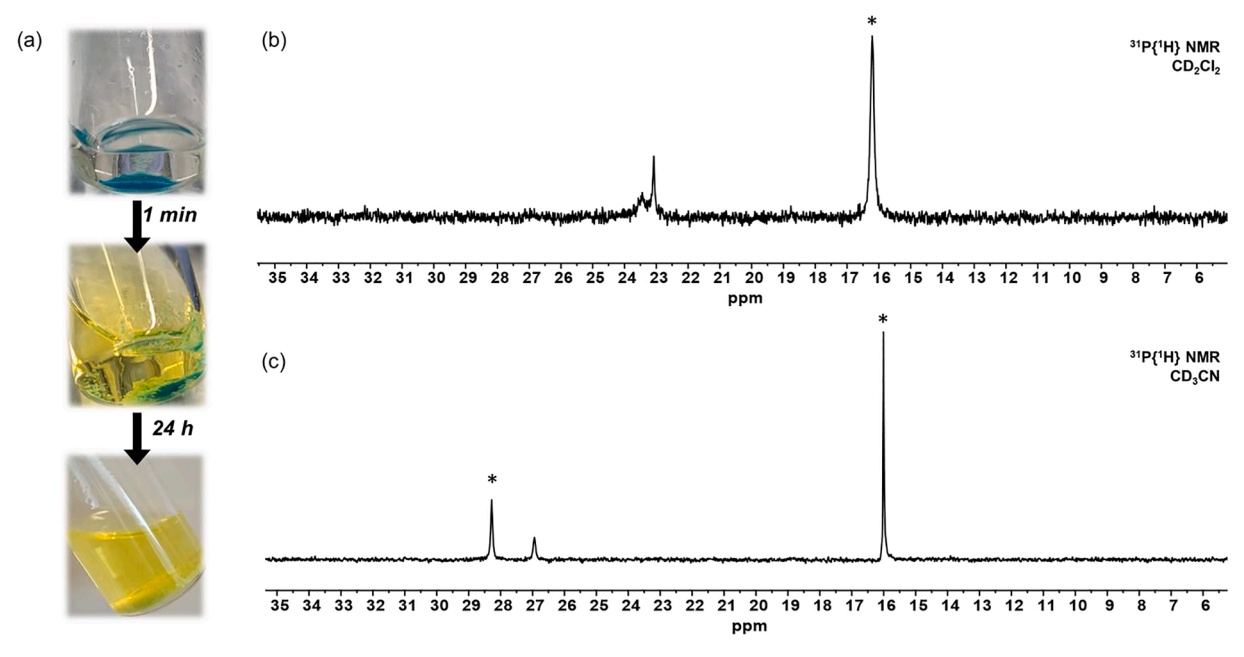


Fig. 5. Crystals of  $3^{MeCN}$  were exposed to excess  $Cl^-$  ions to induce a structural transformation of the WLA complex node, resulting in disassembly of the linear coordination polymer. (a) Within one minute of exposure to a  $Cl^-$  ion solution, crystals of  $3^{MeCN}$  begin to swell and transform into a white powder. Allowing this mixture to stand for 24 h results in complete reaction of  $3^{MeCN}$ . (b)  ${}^{31}P{}^{1}H}$  NMR spectrum of the white solid obtained after 24 h. (c) ${}^{31}P{}^{1}H}$  NMR spectrum of the yellow supernate showing a mixture of  $2^{2Cl}$ ,  $2^{2MeCN}$ , and other products in  $CD_3CN$ . Asterisks denote assigned species. (For interpretation of the references to colour in this figure legend, the reader is referred to the web version of this article.)

## 4. Conclusions

We have reported the first three crystallographically characterized WLA-ICPs. Importantly, we have demonstrated that in their closed state and in the absence of chemical effectors, WLA coordination complexes are rigid enough to form extended crystalline solids. The subsequent introduction of WLA chemical effectors to the crystals allows for their disassembly to molecular components. Thus, one can control macroscale molecular assembly via the structural state of the nanoscale WLA monomer complex. The structural insight gained through X-ray

diffraction will permit the design and synthesis of future WLA-ICP materials, and our structural and chemical analysis has highlighted that appropriate coordination strength should be considered when using WLA complexes to prepare stimuli-responsive extended structures.

## CRediT authorship contribution statement

**Benjamin D. Coleman:** Conceptualization, Investigation, Writing – original draft, Writing – review & editing. **Andrea I. d'Aquino:** Conceptualization, Investigation. **Zachary Kean:** Conceptualization,

Fig. 6. Fully open congeners of 2,  $2^{2Cl}$  and  $2^{2MeCN}$ .

Investigation. Yihan Wang: Validation, Resources. Jenny K. Hedlund Orbeck: Writing – original draft, Writing – review & editing. Charlotte L. Stern: Formal analysis. Chad A. Mirkin: Supervision, Project administration.

### **Declaration of Competing Interest**

The authors declare that they have no known competing financial interests or personal relationships that could have appeared to influence the work reported in this paper.

### Data availability

Data will be made available on request.

## Acknowledgements

This material is based upon work supported by the National Science Foundation under grant CHE-1709888. A.I.d'A. acknowledges a National Science Foundation Graduate Research Fellowship (DGE-1324585). This work made use of the IMSERC X-ray and Mass Spectroscopy Facility at Northwestern University, which has received support from the Soft and Hybrid Nanotechnology Experimental (SHyNE) Resource (NSF ECCS-1542205; NSF ECCS-2025633), the State of Illinois, the International Institute for Nanotechnology (IIN), and Northwestern University.

We thank Dr. Ho Fung Cheng, Dr. Peter T. Smith, Prof. Yuwei Gu, and Prof. Benjamin E. Partridge for their helpful discussions and suggestions. We thank Wenjie Zhou for help with the figures.

#### Appendix A. Supplementary data

CCDC 2176730, CCDC 2176731, and CCDC 2176732 contain the supplementary crystallographic data for 3<sup>MeCN</sup>, 3<sup>DMF</sup>, and 3<sup>H<sub>2</sub>O</sup>, respectively. These data can be obtained free of charge via https://www.ccdc.cam.ac.uk/structures/, or from the Cambridge Crystallographic Data Centre, 12 Union Road, Cambridge CB2 1EZ, UK; fax: (+44) 1223-336-033; or e-mail: deposit@ccdc.cam.ac.uk. Supplementary data to this article can be found online at https://doi.org/10.1016/j.poly.2022.116116.

## References

- [1] J.-P. Changeux, S.J. Edelstein, Allosteric Receptors after 30 Years, Neuron 21 (5) (1998) 959–980, https://doi.org/10.1016/s0896-6273(00)80616-9.
- [2] J.P. Changeux, S.J. Edelstein, Allosteric mechanisms of signal transduction, Science 308 (5727) (2005) 1424–1428, https://doi.org/10.1126/science.1108595.
- [3] N.M. Goodey, S.J. Benkovic, Allosteric regulation and catalysis emerge via a common route, Nat. Chem. Biol. 4 (8) (2008) 474–482, https://doi.org/10.1038/ nchembio 98
- [4] H.N. Motlagh, J.O. Wrabl, J. Li, V.J. Hilser, The ensemble nature of allostery, Nature 508 (7496) (2014) 331–339, https://doi.org/10.1038/nature13001.
- [5] T.R. Cook, Y.R. Zheng, P.J. Stang, Metal-organic frameworks and self-assembled supramolecular coordination complexes: comparing and contrasting the design, synthesis, and functionality of metal-organic materials, Chem. Rev. 113 (1) (2013) 734–777, https://doi.org/10.1021/cr3002824.
- [6] T.R. Cook, P.J. Stang, Recent developments in the preparation and chemistry of metallacycles and metallacages via coordination, Chem. Rev. 115 (15) (2015) 7001–7045, https://doi.org/10.1021/cr5005666.
- [7] M. Albrecht, Dicatechol ligands: novel building-blocks for metallo-supramolecular chemistry, Chem. Soc. Rev. 27 (4) (1998) 281–287, https://doi.org/10.1039/ a8272817
- [8] D.L. Caulder, K.N. Raymond, The rational design of high symmetry coordination clusters, J. Chem. Soc., Dalton Trans. 8 (1999) 1185–1200, https://doi.org/ 10.1039/a808370c.
- [9] D.L. Caulder, K.N. Raymond, Supermolecules by design, Acc. Chem. Res. 32 (11) (1999) 975–982. https://doi.org/10.1021/ar970224v.
- [10] R. Chakrabarty, P.S. Mukherjee, P.J. Stang, Supramolecular coordination: self-assembly of finite two- and three-dimensional ensembles, Chem. Rev. 111 (11) (2011) 6810–6918, https://doi.org/10.1021/cr200077m.
- [11] T.R. Cook, P.J. Stang, Coordination-driven supramolecular macromolecules via the directional bonding approach, Springer International Publishing (2013) 229–248.
- [12] J.A. Faiz, V. Heitz, J.P. Sauvage, Design and synthesis of porphyrin-containing catenanes and rotaxanes, Chem. Soc. Rev. 38 (2) (2009) 422–442, https://doi.org/ 10.1039/b710908n.

- [13] S.J. Lee, W. Lin, Chiral metallocycles: rational synthesis and novel applications, Acc. Chem. Res. 41 (4) (2008) 521–537, https://doi.org/10.1021/ar700216n.
- [14] J.M. Lehn, Perspectives in chemistry-steps towards complex matter, Angew. Chem., Int. Ed Engl. 52 (10) (2013) 2836–2850, https://doi.org/10.1002/anie.201208397.
- [15] T.K. Ronson, S. Zarra, S.P. Black, J.R. Nitschke, Metal-organic container molecules through subcomponent self-assembly, Chem. Commun. (Cambridge, U. K.) 49 (25) (2013) 2476–2490, https://doi.org/10.1039/c2cc36363a.
- [16] S.R. Seidel, P.J. Stang, High-symmetry coordination cages via self-assembly, Acc. Chem. Res. 35 (11) (2002) 972–983, https://doi.org/10.1021/ar010142d.
- [17] M.M. Smulders, I.A. Riddell, C. Browne, J.R. Nitschke, Building on architectural principles for three-dimensional metallosupramolecular construction, Chem. Soc. Rev. 42 (4) (2013) 1728–1754, https://doi.org/10.1039/c2cs35254k.
- [18] Z.J. Wang, K.N. Clary, R.G. Bergman, K.N. Raymond, F.D. Toste, A supramolecular approach to combining enzymatic and transition metal catalysis, Nat. Chem. 5 (2) (2013) 100–103, https://doi.org/10.1038/nchem.1531.
- [19] F. Wurthner, C.C. You, C.R. Saha-Moller, Metallosupramolecular squares: from structure to function, Chem. Soc. Rev. 33 (3) (2004) 133–146, https://doi.org/ 10.1039/b300512g.
- [20] X. Yan, T.R. Cook, J.B. Pollock, P. Wei, Y. Zhang, Y. Yu, F. Huang, P.J. Stang, Responsive supramolecular polymer metallogel constructed by orthogonal coordination-driven self-assembly and host/guest interactions, J. Am. Chem. Soc. 136 (12) (2014) 4460–4463, https://doi.org/10.1021/ja412249k.
- [21] X. Yan, S. Li, J.B. Pollock, T.R. Cook, J. Chen, Y. Zhang, X. Ji, Y. Yu, F. Huang, P. J. Stang, Supramolecular polymers with tunable topologies via hierarchical coordination-driven self-assembly and hydrogen bonding interfaces, Proc. Natl. Acad. Sci. U.S.A. 110 (39) (2013) 15585–15590, https://doi.org/10.1073/pngs.1307472110
- [22] M. Yoshizawa, J.K. Klosterman, M. Fujita, Functional molecular flasks: new properties and reactions within discrete, self-assembled hosts, Angew. Chem., Int. Ed. Engl. 48 (19) (2009) 3418–3438, https://doi.org/10.1002/anie.200805340.
- [23] J.R. Farrell, C.A. Mirkin, I.A. Guzei, L.M. Liable-Sands, A.L. Rheingold, The weaklink approach to the synthesis of inorganic macrocycles, Angew. Chem., Int. Ed.

- Engl. 37 (4) (1998) 465–467, https://doi.org/10.1002/(SICI)1521-3773 (19980302)37:4<465::AID-ANIE465>3.0.CO;2-A.
- [24] R.D. Kennedy, C.W. Machan, C.M. McGuirk, M.S. Rosen, C.L. Stern, A.A. Sarjeant, C.A. Mirkin, General strategy for the synthesis of rigid weak-link approach platinum(II) complexes: tweezers, triple-layer complexes, and macrocycles, Inorg. Chem. 52 (10) (2013) 5876–5888, https://doi.org/10.1021/ic302855f.
- [25] A.M. Lifschitz, M.S. Rosen, C.M. McGuirk, C.A. Mirkin, Allosteric supramolecular coordination constructs, J. Am. Chem. Soc. 137 (23) (2015) 7252–7261, https:// doi.org/10.1021/jacs.5b01054.
- [26] F.M. Dixon, A.H. Eisenberg, J.R. Farrell, C.A. Mirkin, L.M. Liable-Sands, A. L. Rheingold, Neutral macrocycles via halide-induced ring opening of binuclear condensed intermediates, Inorg. Chem. 39 (16) (2000) 3432–3433, https://doi.org/10.1021/ic0000620
- [27] M.V. Ovchinnikov, B.J. Holliday, C.A. Mirkin, L.N. Zakharov, A.L. Rheingold, Threefold symmetric trimetallic macrocycles formed via the Weak-Link Approach, Proc. Natl. Acad. Sci. U.S.A. 99 (8) (2002) 4927–4931, https://doi.org/10.1073/ page 072690599
- [28] P.A. Ulmann, C.A. Mirkin, A.G. DiPasquale, L.M. Liable-Sands, A.L. Rheingold, Reversible ligand pairing and sorting processes leading to heteroligated palladium (II) complexes with hemilabile ligands, Organometallics 28 (4) (2009) 1068–1074, https://doi.org/10.1021/om801060m.
- [29] P.A. Ulmann, A.M. Brown, M.V. Ovchinnikov, C.A. Mirkin, A.G. DiPasquale, A. L. Rheingold, Spontaneous formation of heteroligated Pt<sup>II</sup> complexes with chelating hemilabile ligands, Chem.-Eur. J. 13 (16) (2007) 4529–4534, https://doi.org/10.1002/chem.200601837.
- [30] Y. Liu, Z.S. Kean, A.I. d'Aquino, Y.D. Manraj, J. Mendez-Arroyo, C.A. Mirkin, Palladium(II) Weak-Link approach complexes bearing hemilabile N-heterocyclic carbene-thioether ligands, Inorg. Chem. 56 (10) (2017) 5902–5910, https://doi. org/10.1021/acs.inorgchem.7b00543.
- [31] B.J. Holliday, J.R. Farrell, C.A. Mirkin, K.C. Lam, A.L. Rheingold, Metal-directed assembly of triple-layered fluorescent metallocyclophanes, J. Am. Chem. Soc. 121 (26) (1999) 6316–6317, https://doi.org/10.1021/ja991140f.
- [32] J.R. Farrell, A.H. Eisenberg, C.A. Mirkin, I.A. Guzei, L.M. Liable-Sands, C. D. Incarvito, A.L. Rheingold, C.L. Stern, Templated formation of binuclear macrocycles via hemilabile ligands, Organometallics 18 (23) (1999) 4856–4868, https://doi.org/10.1021/om990585+.
- [33] A.H. Eisenberg, F.M. Dixon, C.A. Mirkin, C.L. Stern, C.D. Incarvito, A.L. Rheingold, Binuclear palladium macrocycles synthesized via the weak-link approach, Organometallics 20 (10) (2001) 2052–2058, https://doi.org/10.1021/om001042z.
- [34] B.J. Holliday, Y.M. Jeon, C.A. Mirkin, C.L. Stern, C.D. Incarvito, L.N. Zakharov, R. D. Sommer, A.L. Rheingold, Probing the mechanistic and energetic basis for the weak-link approach to supramolecular coordination complexes, Organometallics 21 (26) (2002) 5713–5725, https://doi.org/10.1021/om020739c.
- [35] M.S. Masar 3rd, M.V. Ovchinnikov, C.A. Mirkin, L.N. Zakharov, A.L. Rheingold, Fine-tuning the weak-link approach: effect of ligand electron density on the formation of rhodium(I) and iridium(I) metallomacrocycles, Inorg. Chem. 42 (21) (2003) 6851–6858, https://doi.org/10.1021/ic034393p.
- [36] C.A. Sassano, C.A. Mirkin, Degenerate exchange-reactions-a novel and general way to determine the thermodynamic perturbations on transition-metal complexes that result from ligand oxidation, J. Am. Chem. Soc. 117 (45) (1995) 11379–11380, https://doi.org/10.1021/ia00150a052.
- [37] E.T. Singewald, C.A. Mirkin, C.L. Stern, A redox-switchable hemilabile ligand: electrochemical control of the coordination environment of a Rh<sup>1</sup> complex, Angew. Chem., Int. Ed. Engl. 34 (15) (1995) 1624–1627, https://doi.org/10.1002/ pnie 100516241
- [38] E.T. Singewald, X.B. Shi, C.A. Mirkin, S.J. Schofer, C.L. Stern, Novel hemilabile (phosphinoalkyl)arene ligands: mechanistic investigation of all unusual intramolecular, arene-arene exchange reaction, *Organometallics* 15 (13) (1996) 3062–3069, https://doi.org/10.1021/om960114c.
- [39] A.M. Allgeier, C.S. Slone, C.A. Mirkin, L.M. LiableSands, G.P.A. Yap, A. L. Rheingold, Electrochemically controlling ligand binding affinity for transition metals via RHLs: the importance of electrostatic effects, J. Am. Chem. Soc. 119 (3) (1997) 550–559, https://doi.org/10.1021/ja963008a.
- [40] C.S. Slone, C.A. Mirkin, G.P.A. Yap, I.A. Guzei, A.L. Rheingold, Oxidation-state-dependent reactivity and catalytic properties of a Rh(I) complex formed from a redox-switchable hemilabile ligand, J. Am. Chem. Soc. 119 (44) (1997) 10743–10753, https://doi.org/10.1021/ja9723601.
- [41] I.V. Kourkine, C.S. Slone, C.A. Mirkin, L.M. Liable-Sands, A.L. Rheingold, Small molecule-induced intramolecular electron "pitch and catch" in a rhodium(I) complex with substitutionally inert redox-active ligands, Inorg. Chem. 38 (12) (1999) 2758–2759, https://doi.org/10.1021/ic990193v.
- [42] A.M. Allgeier, E.T. Singewald, C.A. Mirkin, C.L. Stern, [Rh(η<sup>4</sup>-(η/<sup>5</sup>-C<sub>5</sub>H<sub>4</sub>)OCH<sub>2</sub>CH<sub>2</sub>P (C<sub>6</sub>H<sub>5</sub>)<sub>2</sub>)<sub>2</sub>Fe)]BF<sub>4</sub>: an olefin hydrogenation catalyst and the first rhodium(I) cisphosphine-cis-ether complex characterized by single-crystal X-ray diffraction methods, Organometallics 13 (8) (2002) 2928–2930, https://doi.org/10.1021/om000203005
- [43] H.F. Cheng, A.I. d'Aquino, J. Barroso-Flores, C.A. Mirkin, A Redox-switchable, allosteric coordination complex, J. Am. Chem. Soc. 140 (44) (2018) 14590–14594, https://doi.org/10.1021/jacs.8b09321.
- [44] A.M. Lifschitz, C.M. Shade, A.M. Spokoyny, J. Mendez-Arroyo, C.L. Stern, A. A. Sarjeant, C.A. Mirkin, Boron-dipyrromethene-functionalized hemilabile ligands as "turn-on" fluorescent probes for coordination changes in weak-link approach complexes, Inorg. Chem. 52 (9) (2013) 5484–5492, https://doi.org/10.1021/ic400383t.

- [45] Y. Liu, J. Zhou, M.R. Wasielewski, H. Xing, C.A. Mirkin, A four-state fluorescent molecular switch, Chem. Commun. (Cambridge, U. K.) 54 (85) (2018) 12041–12044, https://doi.org/10.1039/c8cc05159c.
- [46] N.C. Gianneschi, S.T. Nguyen, C.A. Mirkin, Signal amplification and detection via a supramolecular allosteric catalyst, J. Am. Chem. Soc. 127 (6) (2005) 1644–1645, https://doi.org/10.1021/ja0437306.
- [47] H.J. Yoon, C.A. Mirkin, PCR-like cascade reactions in the context of an allosteric enzyme mimic, J. Am. Chem. Soc. 130 (35) (2008) 11590–11591, https://doi.org/ 10.1021/ja804076q.
- [48] H.J. Yoon, J. Kuwabara, J.H. Kim, C.A. Mirkin, Allosteric supramolecular triple-layer catalysts, Science 330 (6000) (2010) 66–69, https://doi.org/10.1126/science 1193028
- [49] C.M. McGuirk, J. Mendez-Arroyo, A.M. Lifschitz, C.A. Mirkin, Allosteric regulation of supramolecular oligomerization and catalytic activity via coordination-based control of competitive hydrogen-bonding events, J. Am. Chem. Soc. 136 (47) (2014) 16594–16601, https://doi.org/10.1021/ja508804n.
- [50] A.M. Lifschitz, R.M. Young, J. Mendez-Arroyo, C.L. Stern, C.M. McGuirk, M. R. Wasielewski, C.A. Mirkin, An allosteric photoredox catalyst inspired by photosynthetic machinery, Nat. Commun. 6 (1) (2015) 6541, https://doi.org/10.1038/ncomms7541.
- [51] A.M. Lifschitz, R.M. Young, J. Mendez-Arroyo, C.M. McGuirk, M.R. Wasielewski, C. A. Mirkin, Cooperative electronic and structural regulation in a bioinspired allosteric photoredox catalyst, Inorg. Chem. 55 (17) (2016) 8301–8308, https://doi.org/10.1021/acs.inorgchem.6b00095.
- [52] F. Bigdeli, C.T. Lollar, A. Morsali, H.C. Zhou, Switching in metal-organic frameworks, Angew. Chem., Int. Ed. Engl. 59 (12) (2020) 4652–4669, https://doi. org/10.1002/anie.201900666.
- [53] S. Kitagawa, K. Uemura, Dynamic porous properties of coordination polymers inspired by hydrogen bonds, Chem. Soc. Rev. 34 (2) (2005) 109–119, https://doi. org/10.1039/b313997m.
- [54] A.J. McConnell, C.S. Wood, P.P. Neelakandan, J.R. Nitschke, Stimuli-responsive metal-ligand assemblies, Chem. Rev. 115 (15) (2015) 7729–7793, https://doi.org/ 10.1021/cr500632f.
- [55] A.I. d'Aquino, Z.S. Kean, C.A. Mirkin, Infinite coordination polymer particles composed of stimuli responsive coordination complex subunits, Chem. Mater. 29 (24) (2017) 10284–10288, https://doi.org/10.1021/acs.chemmater.7b03638.
- [56] C.W. Tate, A.D. Gee, R. Vilar, A.J.P. White, N.J. Long, Reversible carbon monoxide binding at copper(I) P-S-X (X = N, O) coordination polymers, J. Organomet. Chem. 715 (2012) 39–42, https://doi.org/10.1016/j.jorganchem.2012.05.032.
- [57] M.S. Rosen, C.L. Stern, C.A. Mirkin, Heteroligated Pt<sup>II</sup> weak-link approach complexes using hemilabile N-heterocyclic carbene-thioether and phosphinothioether ligands, Chem. Sci. 4 (11) (2013) 4193, https://doi.org/10.1039/ c3sc51557e.
- [58] J. Mendez-Arroyo, J. Barroso-Flores, A.M. Lifschitz, A.A. Sarjeant, C.L. Stern, C. A. Mirkin, A multi-state, allosterically-regulated molecular receptor with switchable selectivity, J. Am. Chem. Soc. 136 (29) (2014) 10340–10348, https://doi.org/10.1021/ja503506a.
- [59] A.M. Lifschitz, R.M. Young, J. Mendez-Arroyo, V.V. Roznyatovskiy, C.M. McGuirk, M.R. Wasielewski, C.A. Mirkin, Chemically regulating Rh(I)-bodipy photoredox switches, Chem. Commun. (Cambridge U.K.) 50 (52) (2014) 6850–6852, https://doi.org/10.1039/c4cc01345i.
- [60] G. Sheldrick, ShelXT: integrating space group determination and structure solution, Acta Crystallogr. A 70 (2014) C1437–C, https://doi.org/10.1107/ S2053273314085623
- [61] O.V. Dolomanov, L.J. Bourhis, R.J. Gildea, J.A.K. Howard, H. Puschmann, Olex2: A complete structure solution, refinement and analysis program, J. Appl. Crystallogr. 42 (2009) 339–341, https://doi.org/10.1107/S0021889808042726.
- [62] G.M. Sheldrick, Crystal structure refinement with ShelXL, Acta Crystallogr. C 71 (2015) 3–8, https://doi.org/10.1107/S2053229614024218.
- [63] V. Balogh-Hergovich, G. Speier, Reaction of copper(I) chloride pyridine complexes with dioxygen. A kinetic study, Transition Met. Chem. 7 (3) (1982) 177–180, https://doi.org/10.1007/bf01035837.
- [64] M.T. Rodgers, J.R. Stanley, R. Amunugama, Periodic trends in the binding of metal ions to pyridine studied by threshold collision-induced dissociation and density functional theory, J. Am. Chem. Soc. 122 (44) (2000) 10969–10978, https://doi. org/10.1021/ja0027923.
- [65] R. Dobrawa, P. Ballester, C.R. Saha-Möller, F. Würthner, Thermodynamics of 2,2': 6',2"-terpyridine-metal ion complexation, in: Metal-Containing and Metallosupramolecular Polymers and Materials, American Chemical Society, 2006, pp. 43–62.
- [66] S.R. Batten, J.C. Jeffery, M.D. Ward, Studies of the construction of coordination polymers using linear pyridyl-donor ligands, Inorg. Chim. Acta 292 (2) (1999) 231–237, https://doi.org/10.1016/S0020-1693(99)00203-0.
- [67] M. Du, X.H. Bu, Y.M. Guo, H. Liu, S.R. Batten, J. Ribas, T.C. Mak, First Cu(II) diamondoid net with 2-fold interpenetrating frameworks. the role of anions in the construction of the supramolecular arrays, Inorg. Chem. 41 (19) (2002) 4904–4908, https://doi.org/10.1021/ic025559+.
- [68] R. Kitaura, K. Fujimoto, S.-I. Noro, M. Kondo, S. Kitagawa, A Pillared-layer coordination polymer network displaying hysteretic sorption: [Cu<sub>2</sub>(Pzdc)<sub>2</sub>(Dpyg)]<sub>n</sub> (Pzdc= Pyrazine-2,3-Dicarboxylate; Dpyg=1,2-Di(4-Pyridyl)Glycol), Angew. Chem., Int. Ed. Engl. 41 (1) (2002) 133–135, https://doi.org/10.1002/1521-3773 (20020104)41:1<133::Aid-anie133>3.0.Co;2-r.
- [69] B. Rather, M.J.A. Zaworotko, 3d metal-organic network, [Cu<sub>2</sub>(glutarate)<sub>2</sub>(4,4'-bipyridine)], that exhibits single-crystal to single-crystal dehydration and rehydration, Chem. Commun. (Cambridge U.K.) 7 (2003) 830–831, https://doi.org/10.1039/b301219k.

- [70] M.L. Tong, L.J. Li, K. Mochizuki, H.C. Chang, X.M. Chen, Y. Li, S. Kitagawa, A novel three-dimensional coordination polymer constructed with mixed-valence dimeric copper(I, II) units, Chem. Commun. (Cambridge U.K.) 3 (2003) 428–429, https://doi.org/10.1039/b210914j.
- [71] W. Mori, S. Takamizawa, C.N. Kato, T. Ohmura, T. Sato, Molecular-level design of efficient microporous materials containing metal carboxylates: inclusion complex formation with organic polymer, gas-occlusion properties, and catalytic activities for hydrogenation of olefins, Microporous Mesoporous Mater. 73 (1–2) (2004) 31–46, https://doi.org/10.1016/j.micromeso.2004.02.019.
- [72] J. Park, J.R. Li, Y.P. Chen, J. Yu, A.A. Yakovenko, Z.U. Wang, L.B. Sun, P. B. Balbuena, H.C. Zhou, A versatile metal-organic framework for carbon dioxide
- capture and cooperative catalysis, Chem. Commun. (Cambridge U.K.) 48 (80) (2012) 9995–9997, https://doi.org/10.1039/c2cc34622b.
- [73] M. Yoon, R. Srirambalaji, K. Kim, Homochiral metal-organic frameworks for asymmetric heterogeneous catalysis, Chem. Rev. 112 (2) (2012) 1196–1231, https://doi.org/10.1021/cr2003147.
- [74] A. del Zotto, A. Mezzetti, P. Rigo, M. Bressan, F. Morandini, A. Morvillo, Synthesis and NMR studies of palladium(II) and platinum(II) complexes with hybrid bidentate ligands Ph<sub>2</sub>P(CH<sub>2</sub>)<sub>2</sub>SR, Inorg. Chim. Acta 158 (2) (1989) 151–158, https://doi.org/10.1016/s0020-1693(00)80828-2.